



# Effect of fluorine doping on the improvement of electrical and photocatalytic properties of ZnO films

Seniye Karakaya<sup>1</sup> · Leyla Kaba<sup>1</sup>

Received: 23 November 2023 / Accepted: 15 January 2024 / Published online: 14 February 2024  
© The Author(s) 2024

## Abstract

ZnO:F thin films were produced by ultrasonic spray pyrolysis (USP) technique. For photovoltaic and photocatalytic applications, the properties of ZnO films have been tried to be improved by adding the fluorine (F) element. The average optical transmittance was higher than 85%. Photoluminescence (PL) spectra depict blue, green and yellow emission in deposited films. Photocatalytic activity of ZnO and ZnO:F thin films was evaluated with methylene blue (MB) organic pollutant under UV irradiation. 5% doped ZnO:F film successfully decomposed ~80% using MB as photocatalyst. The lowest resistivity ( $3.54 \times 10^{-3} \Omega\text{cm}$ ), high carrier concentration ( $2.52 \times 10^{20} \text{cm}^{-3}$ ) and high hall mobility ( $8.28 \text{cm}^2\text{V}^{-1} \text{s}^{-1}$ ) were observed in ZnO:F (5%) film. With this study, it was concluded that F-doped ZnO films were effective in the degradation of MB, which is widely used in the food and pollutant industries. Therefore, it makes ZnO:F films a promising material in both optoelectronic and photocatalytic applications due to their optimum properties.

**Keywords** F-doped ZnO · USP technique · Methylene blue · Photocatalytic · Hall effect

## 1 Introduction

One of the most abundant clean energy sources in the world is solar energy. Photocatalysis is an effective method to break down pollutants using inexhaustible and clean solar energy. Photocatalysis, which uses semiconductor oxide photocatalysts to perform pollutant photodegradation in wastewater, can reduce the concentration of dangerous organic compounds in water and has a field of use due to this feature [1]. Among the photocatalytic materials, oxide semiconductors such as titanium oxide ( $\text{TiO}_2$ ) and zinc oxide (ZnO) have attracted great interest as photocatalysts in recent years due to their easy availability and low toxicity [2]. ZnO has higher photocatalytic activity than  $\text{TiO}_2$ , it is efficient, economical, environmentally friendly and stable [3].

To improve and change the different properties (morphological, structural, optical and electrical properties) of ZnO in optoelectronic applications [4], solar cells [5], gas sensing [6], light-emitting diodes (LEDs) [7] and photocatalysis [8], it is very convenient to add elements such as cationic

elements Mg [9], Li [10] or anionic elements Cl [11], F [12], Br [13]. Fluorine (F) is one of the most suitable n-type anionic additives used to improve some physical properties of ZnO thin films. Owing to the strong electronegativity (3.98) and ionic radius of F (0.136 nm), that is similar to that of  $\text{O}_2$  (0.140 nm), F atoms can be replaced into O sites [14]. Many researchers have studied F-doped ZnO films prepared with different production techniques [14–19]. However, from the literature, there is scarcely any work done on the photocatalytic properties of fluorine-doped ZnO thin films. The studies carried out on photocatalytic are summarized in Table 1. As can be seen from Table 1, the number of studies on the photocatalytic activity of F-doped ZnO films/nanostructures is few, and among them, MB organic dye has never been studied. Galil et al. [20] obtained ZnO:F nanostructured thin films through spray pyrolysis. The photocatalytic activity of ZnO and ZnO:F thin films was also evaluated to purify water from phenol as colorless organic waste by phenol photodegradation under UV irradiation. In this study, fluorine-doped ZnO films with promising results that can be used in optoelectronic and photocatalytic applications were produced by ultrasonic spray pyrolysis (USP) method, which is a low-cost technique. Our aim is to investigate the effect of F-doping on ZnO films to increase the photocatalytic activity. Photocatalytic activity was evaluated by measuring the photocatalytic

✉ Seniye Karakaya  
seniyek@ogu.edu.tr

<sup>1</sup> Department of Physics, Faculty of Science, Eskisehir Osmangazi University, 26040 Eskisehir, Turkey

**Table 1** Reports on the application of photocatalytic degradation of F-doped ZnO

Sample	Production technique	Organic pollutant	Light source	Refs.
ZnO:F	Spray pyrolysis	Methylene blue	9 W/ UV lamp	Present work
ZnO:F	Spray pyrolysis	Phenol	6 W/ Hg lamp	[20]
ZnO:F	Hydrothermal	Diclofenac	10 W/UV-LEDs	[21]
ZnO:F	One-step microwave irradiation	Methyl violet and Rhodamine B	Visible light	[22]
ZnO:F	Hydrothermal	Malachite green	300W/Xenon lamp	[23]
ZnO:F	Sol-gel	Diclofenac	1500 W/Xenon arc lamp	[24]

degradation of the methylene blue aqueous solution. Choosing this pollutant as pollutant molecules is because of the most used and pollutant existing in industrial wastewater.

## 2 Experimental

ZnO thin films were deposited on ultrasonically cleaned glass substrates using the ultrasonic spray pyrolysis (USP) method at various F-doping ratios. The starting solution (0.15 M) zinc acetate dihydrate  $\text{Zn}(\text{CH}_3\text{COO})_2 \cdot 2\text{H}_2\text{O}$  was dissolved in 75 ml of methanol and 25 ml of distilled water (3:1) and stirred at 60 °C for 15 min on a magnetic stirrer. Similarly, (0.05 M) ammonium fluoride ( $\text{NH}_4\text{F}$ ) (5, 10, 15%) was added to the mixture solution. The solution flow rate was kept constant at 5 ml/min and the substrate temperature at  $375 \pm 5$  °C. Air at 1 bar pressure was used as the carrier gas. The photocatalytic testing process of ZnO:F films is given in our previous study [25, 26].

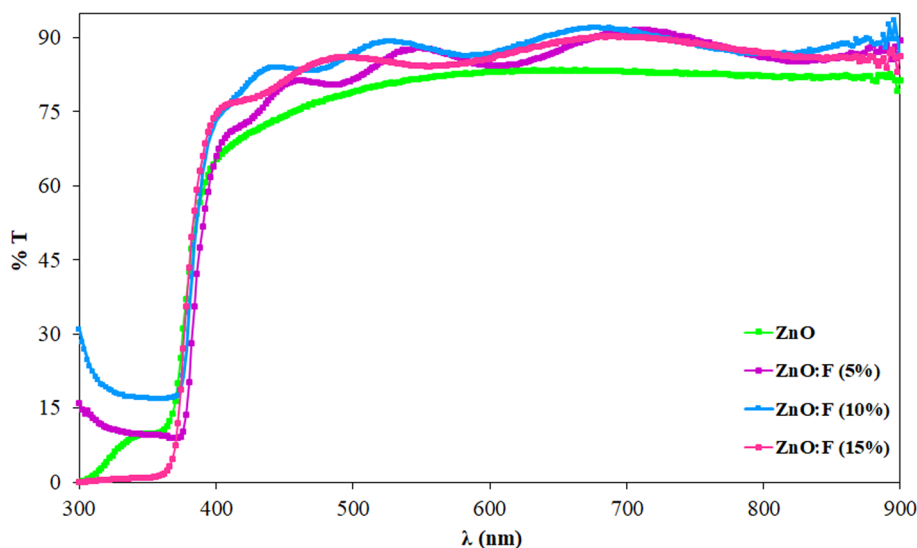
Optical transmittance of the films was performed with UV-Vis spectrophotometer (Perkin Elmer Shimadzu-2550) at 300–900 nm wavelength range. “Panalytical Empyrian” was used for XRD pattern of the ZnO:F films. Photoluminescence (PL) spectra at room temperature were take a by

the Perkin Elmer LS55 Fluorescence Spectrometer using an excitation wavelength of 325 nm. Morphological properties of the films of all films were defined by Field Emission Scanning Electron Microscope (FESEM) images using Hitachi Regulus 8230 device. The resistivity, the Hall mobility and carrier concentration of the ZnO:F films were found out using a Hall effect system (Teknis HLF 1.2 model). The thickness values of the films were determined with the “Digital Coating Thickness Meter (Elcometer)” device.

## 3 Results and discussion

Figure 1 shows the optical transmittance characteristics of the ZnO:F films in the 300–900 nm wavelength region. The thin films are highly transparent in this wavelength range with the value of transmittance ~85–95%. In addition, the transmittance of the film increases significantly when F-doped is added compared to the undoped ZnO film. Thickness values of the ZnO, ZnO:F (5%), ZnO:F (10%) and ZnO:F (15%) films were obtained using Elcometer as 150 nm, 125 nm, 114 nm and 100 nm, respectively. As the thickness values of the films decrease, their transmittance values increase. In Fig. 1, the transmittance curves of

**Fig. 1** The transmittance spectra of ZnO:F films



F-doped ZnO films show a well-defined interference fringe pattern showing the smooth surface of the thin films [27]. This is because incoming photons oscillate between interfaces (air-film-substrate) during measurement producing different transmitted waves, these waves interfere consistently and produce optical interference fringes [28, 29].  $(\alpha h\nu^2 - h\nu)$  plots of undoped and F-doped ZnO films are shown in Fig. 2. The optical band gaps generally decrease due to the band shrinkage effect with increasing carrier concentration. The decrease in the band gap can be attributed to the strong sp-d exchange interaction between the band electrons and localized electrons of the dopant. This situation is also supported by some studies in the literature [30, 31].

Structural properties of the obtained ZnO:F thin films evaluated using XRD analysis. The XRD spectra of the ZnO:F samples are shown in Fig. 3. All XRD diffraction peaks were defined by crosscheck with the JCPDS data file for ZnO:F corresponding to (100), (002), (101), (102), (110), (103) and (112) reflections of the hexagonal wurtzite structure [32]. All ZnO thin films corresponded to the hexagonal wurtzite type ZnO structure and preferred the (002) orientation. The films suggest preferential orientation due to the lowest surface free energy in this direction

(002) [33]. The inclusion of F in the unadulterated ZnO film results in lower intensity and degradation of crystal quality of the XRD peaks of the ZnO:F films. With increasing fluorine doping, the peak intensity of the (002) plane decreased, while the peak intensities of the (100) and (101) planes increased. Penetration of the F ion, which has a smaller ionic radius than oxygen, into the ZnO structure will reduce the crystallization of ZnO films, as it may cause deformation in the lattice due to F doping [17].

From the integral width of the (002) peak and the peak position, the parameters for the crystal size ( $D$ ), macro-strain ( $\langle \epsilon \rangle$ ) and dislocation density ( $\delta$ ) of the films are calculated. The phases assigned by the lattice spacing ( $d$ ), diffraction angle ( $2\theta$ ) and ( $hkl$ ) planes of the films calculated from the (002) peak positions are listed in Table 2. The crystallite size ( $D$ ) is estimated using Scherrer formula [34]

$$D = \frac{k\lambda}{\beta \cos \theta}, \quad (1)$$

where  $k = (0.94)$  is the Scherrer constant,  $\lambda$  is the X-ray wavelength,  $\theta$  is the Bragg angle of the (002) peak, and  $\beta$  is

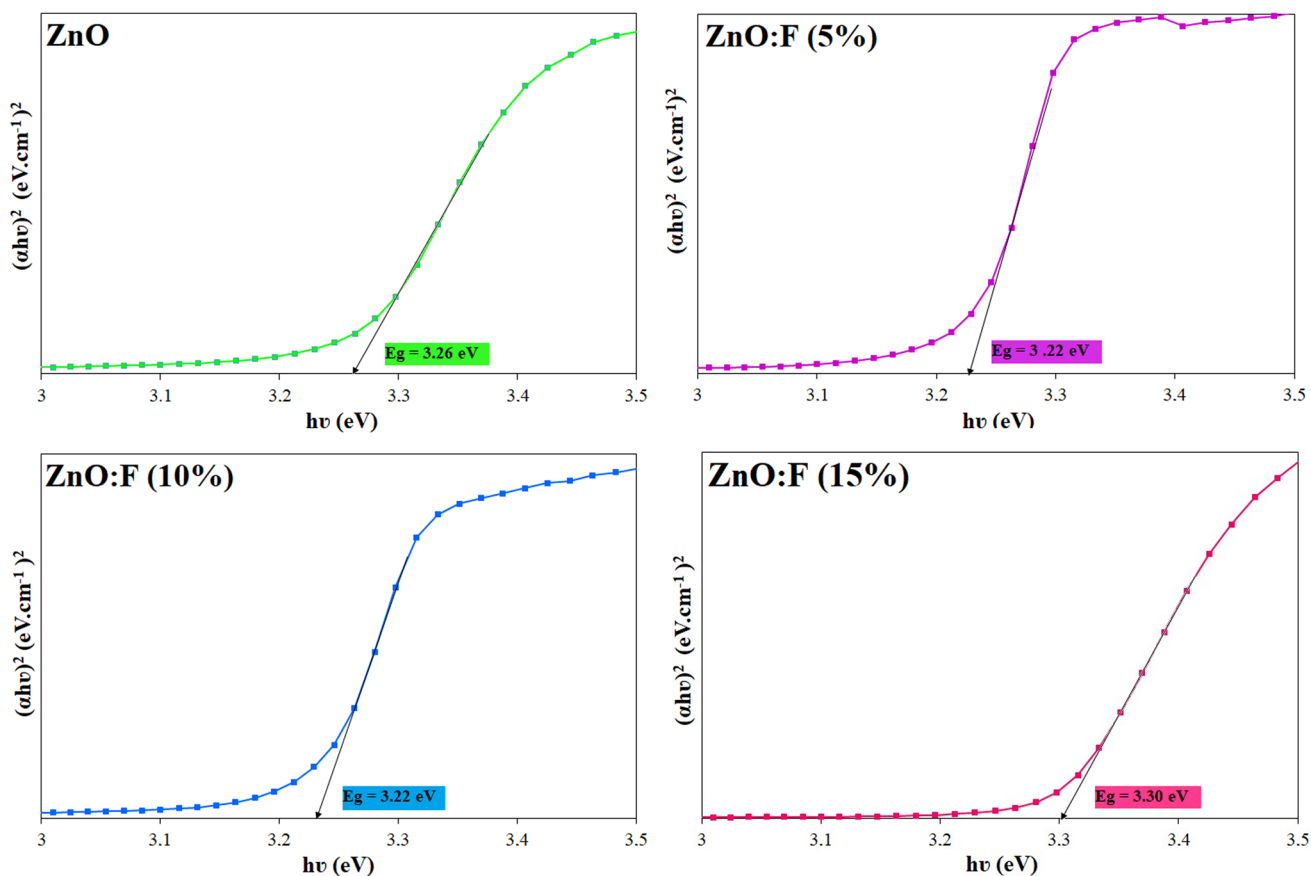


Fig. 2  $(\alpha h\nu^2 - h\nu)$  plots of undoped and F-doped ZnO films

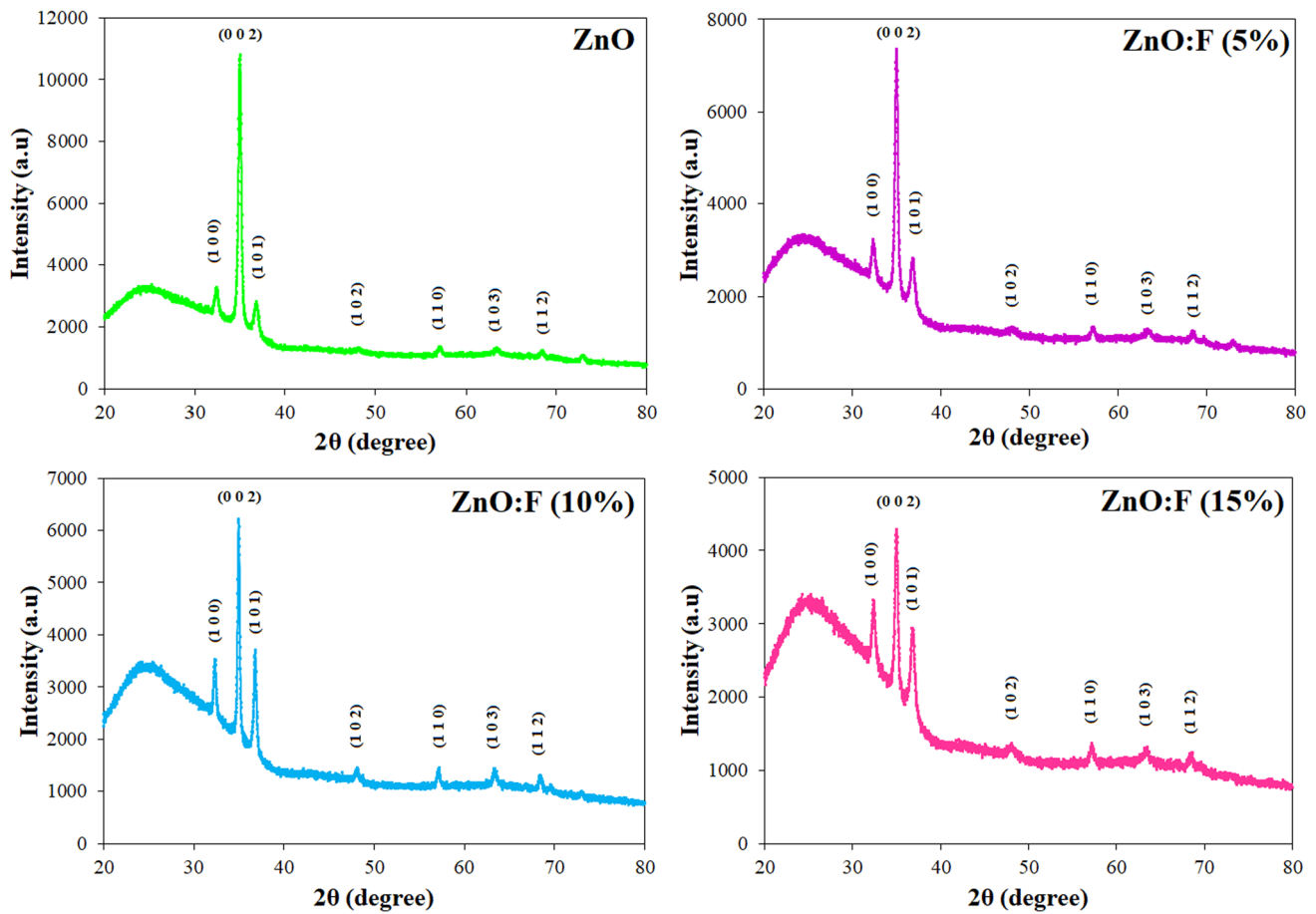


Fig. 3 XRD patterns of ZnO:F films

Table 2 Structural parameters for ZnO:F films

Film	2 (°)	d (Å)	2θ <sub>0</sub> (°)		d <sub>0</sub> (Å) JCPDS	(h k l)
			JCPDS			
ZnO	34.99	2.5616	34.42		2.6033	(0 0 2)
ZnO:F (5%)	34.97	2.5636	34.42		2.6033	(0 0 2)
ZnO:F (10%)	34.99	2.5641	34.42		2.6033	(0 0 2)
ZnO:F (15%)	34.95	2.5647	34.42		2.6033	(0 0 2)

the FWHM value [35]. The macro-strain (<e>) are found by the following equation [36]:

$$\langle e \rangle = \frac{d - d_0}{d_0} \tag{2}$$

δ is an important parameter to find the amount of defects in a crystal. The value of dislocation density (δ) is calculated using the following equation [37]:

Table 3 Variation of crystallite size (D), macro-strain values (<e>) and dislocation density (δ) for the (002) plane of ZnO:F films

Film	D (nm)		<e>	δ × 10 <sup>-4</sup> (1/nm <sup>2</sup> )
	XRD	FESEM		
ZnO	88.6	91	- 0.0160	1.3
ZnO:F (5%)	53.4	51	- 0.0152	3.5
ZnO:F (10%)	43.4	42	- 0.0151	5.3
ZnO:F (15%)	66.6	68	- 0.0148	2.2

$$\delta = \frac{1}{D^2} \tag{3}$$

Parameters such as grain size (crystallite size), macro-strain and dislocation density are shown in Table 3. The increase in the dislocation density indicates the defects generated in the ZnO lattice. Crystallite size F-doped ZnO is lower than undoped ZnO films. The change in crystallite size (D) can be ascribed to the formation of extrinsic defects created by the increase in F doping and can be described on the principle of the Zener pinning effect

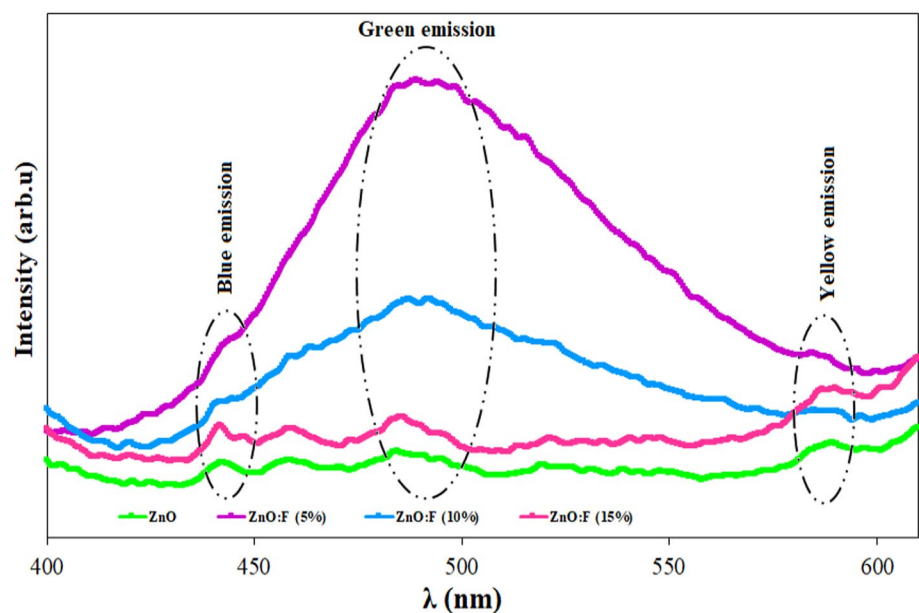
[38]. Because of the zener pinning effect, as the retarding force has greater than the driving force of grain boundary movement caused by specific defects in the ZnO lattice, growth grain is constrained, resulting in a smaller crystallite [39]. The reason for the decrease in crystal size with increasing fluorine percentage can be explained by the fact that fluorine atoms do not replace oxygen atoms, but instead occupy interstitial states leading to a large number of dislocations. This reduction in crystallite size is also consistent with other studies reported in the literature [40].

Emission spectra that obtain information about various defects in the ZnO structure. Figure 4 shows the room temperature PL spectra of ZnO:F films at various doping ratios (0, 5, 10, 15%) under 325 nm wavelength excitation. The emission types observed in the films are blue emission (~440 nm), green emission (~490 nm) and yellow emission (~590 nm), respectively. The blue emission at ~440 nm is attributed to the electronic transition energy between shallow levels of zinc interstitial ( $Zn_i$ ) and acceptor levels of zinc vacancy ( $V_{Zn}$ ) [41, 42]. The green emission peak at ~490 nm is usually due to the recombination of photoexcited holes with electrons occupying the ionized oxygen vacancies [43, 44]. The yellow emission peak observed at ~590 nm is attributed to the oxygen interstitial ( $O_i$ ) [45, 46]. Therefore, the surface morphology and size of the samples also affect the PL properties [47]. The decrease in PL intensity with increasing F contribution in the samples can be attributed to the defect state on the surface. It has been noticed that the PL emission intensity gradually decreases with the gradual increase of F content, as seen in the PL spectrum. In this study, grain size values obtained from FESEM measurements (in Table 3) support this situation.

The surface morphology of ZnO:F (0, 5, 10, 15%) thin films is analyzed by observing FESEM micrographs as shown in Fig. 5. Images in Fig. 5 were taken at 150 K magnification for all films. Surface morphology is an important way for obtaining information about the microstructure of thin films [48]. In the morphology of ZnO:F films, there are nanoparticles consisting of spherical particles and irregular hexagonal-shaped layers [49, 50]. These layers became more prominent with the F element doping. This irregularity in hexagonal plates increases with F doping. While spherical particles appear denser and continuous in undoped ZnO and ZnO:F (15%) films, the structure consisting of irregular hexagonal-shaped layers is dominant, especially in ZnO:F (5%) films. We think that this irregular hexagonal-shaped layer structure increases the active surface area and positively affects the photocatalytic activity of the ZnO:F (5%) film.

The photocatalytic degradation performance of MB for 360 min of UV light exposure every 60 min by all ZnO:F films is shown in Fig. 6. Percent degradation efficiency of ZnO:F films are given in Fig. 7. The time-dependent  $\ln(C_0/C)$  plots in Fig. 8a obey the first-order rate law of photocatalytic degradation. Time-dependent  $\ln(C_0/C)$  graphs and plot of degradation rate constants ( $k$ ) values are given in Fig. 8. Figure 7 shows that the ZnO:F (5%) film has the highest % degradation efficiency and rate constant ( $k$ ). As shown in Fig. 6, because the defect density of the ZnO:F (5%) film is higher than the other films, it increases the photocatalytic activity by preventing e/h recombination. These results are in agreement with the electrical parameters of the films, where low-doping rates of F can greatly improve the concentration of charge carriers and their mobility in the ZnO film. Therefore, in the photocatalytic activity of ZnO films wherein low-doping level of F (5%),  $F^-$  ions can

**Fig. 4** PL spectra of ZnO:F films



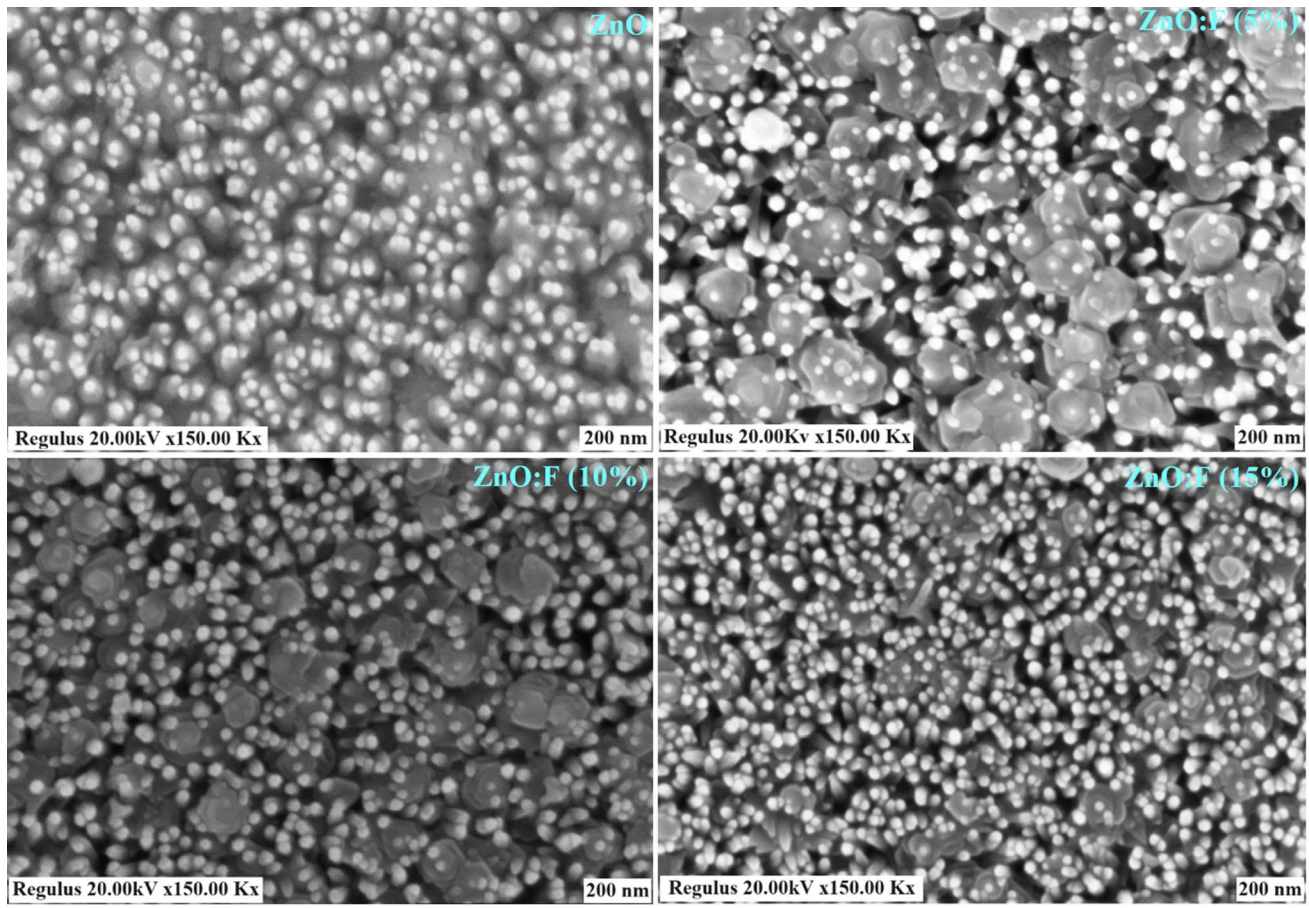


Fig. 5 FESEM images of ZnO:F films

substitutionally occupy the  $O^{2-}$  ions sites and increase the charge carriers in the ZnO [20]. It is seen that this situation is compatible with the carrier concentration values in Table 3. To quantify the rate of degradation, we describe the concentration degradation with one rate constant  $k$  [51]

$$C(t) = C(0)\exp(-kt), \tag{4}$$

where  $C(0)$  is the initial pollutant concentration and  $t$  is the exposure time to UV illumination

$$\ln[C(t) \div C(0)] = -kt. \tag{5}$$

The percent MB degradation rate of ZnO:F thin films was calculated by the following formula [52]:

$$\eta(\% \text{degradation}) = \left(1 - \frac{C_t}{C_0}\right) \times 100, \tag{6}$$

where  $\eta$  (%) notifies the degradation percentage of pollutants.  $C_0$  and  $C_t$ (mg/L) mean the primary concentration and equilibrium concentration of pollutants, respectively.

Electrical properties of F-doped ZnO thin films such as resistivity, Hall mobility and carrier concentration were

characterized by Hall effect measurements. These characterized parameters are summarized in Table 4. Resistivity decreases with F-doping concentration and attains a minimum value of  $3.54 \times 10^{-3} \Omega\text{cm}$  at 5% of F doping. The carrier density increased initially with an increasing F concentration, reaching a peak density of  $1.60 \times 10^{20} \text{ cm}^{-3}$  at 10% F, and then decreased with further increases in F concentration. Therefore, when F replaces O at the O sites, the formation of the Zn–F bonds supplies an excess electron at the Zn site that for this reason increases the carrier concentration of the FZO films. Similar results were recorded in other studies [20, 53]. When Hall effect measurements were evaluated, it was observed that increased mobility and carrier concentration with fluorine contributed positively to the electrical conductivity of ZnO:F films.

### 4 Conclusions

ZnO films, the electrical and photocatalytic properties of which have been improved by F-doping, have been successfully produced using the USP technique. When the films

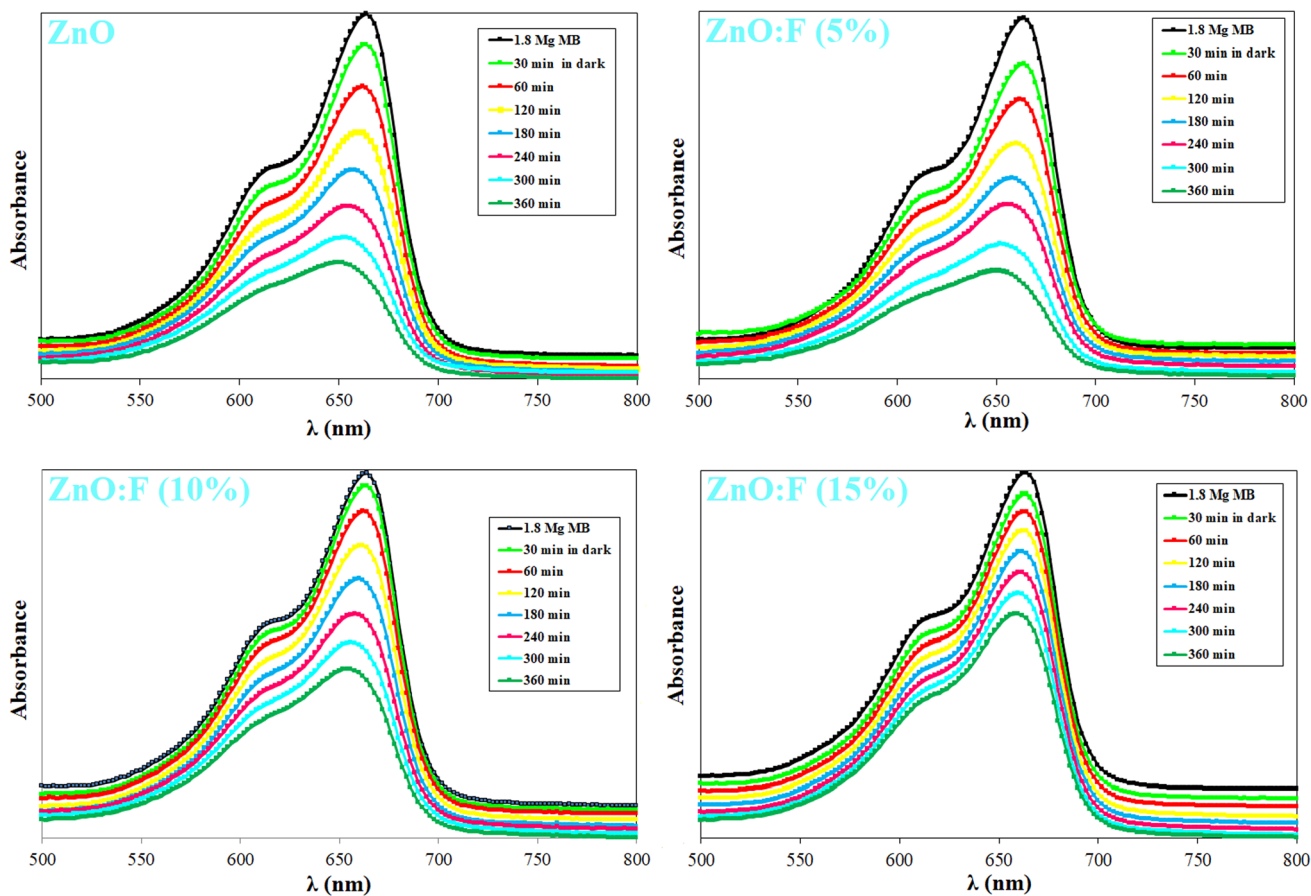


Fig. 6 The absorbance spectra of the MB solution for ZnO:F films

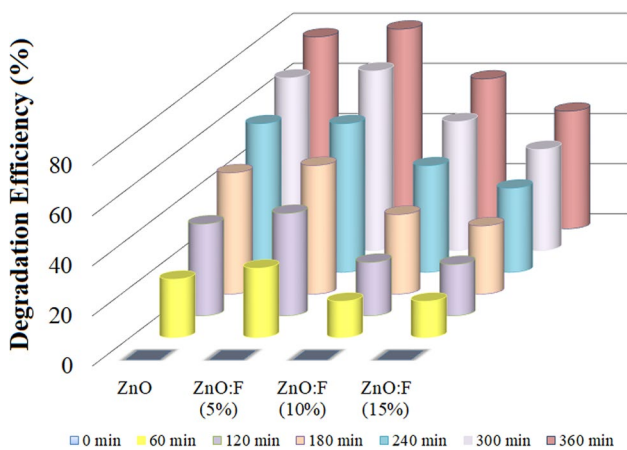
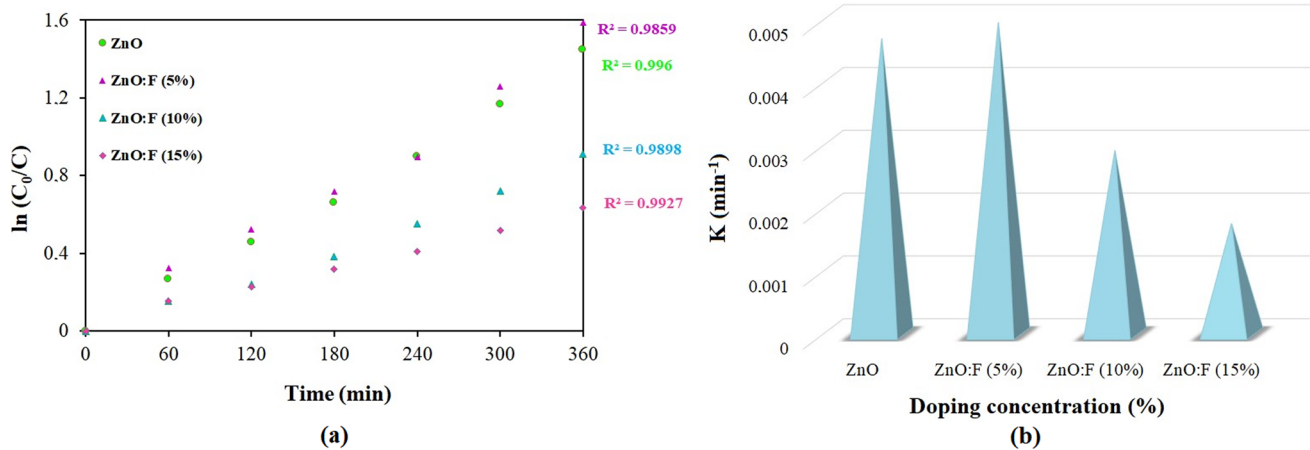


Fig. 7 Graph of the degradation efficiency of ZnO:F thin films

obtained are evaluated in terms of photocatalytic applications; it has been observed that ZnO:F films have structural and morphological properties suitable for degrading water pollutants such as MB pollutant. The nanostructure observed from the FESEM images of the films positively affects the photocatalytic activity by increasing the active surface area. While the photocatalytic degradation rate of undoped ZnO was 76.5%, it increased to ~80% at a 5% doping rate. The fluorine atoms substitution into the ZnO lattice has beneficial results with regard to increasing the carrier concentration. Therefore, these effects improve the electrical properties. Evaluation of all the properties of the films showed that F-doped ZnO thin films have material properties that are useful in photocatalysis applications such as wastewater treatment.



**Fig. 8** **a** Time-dependent  $\ln(C_0/C)$  plot of Methylene Blue solution for ZnO:F films. **b** Plot of degradation rate constants ( $k$ ) of ZnO:F thin-film photocatalysts

**Table 4** Electrical properties of undoped ZnO and ZnO:F films

Film	$\rho$ ( $\Omega$ cm)	$\mu$ ( $\text{cm}^2\text{V}^{-1}\text{s}^{-1}$ )	$n$ ( $\text{cm}^{-3}$ )
ZnO	0,01305039	6,9661	$5,77,176 \times 10^{19}$
ZnO:F (5%)	0,003548523	8,2882	$2,52,549 \times 10^{20}$
ZnO:F (10%)	0,012076754	3,2221	$1,60,596 \times 10^{20}$
ZnO:F (15%)	0,123,734	1,0788	$4,6847 \times 10^{19}$

**Author contributions** SK contributed to conceptualization, writing—review and editing, and supervision. LK: writing and editing.

**Funding** Open access funding provided by the Scientific and Technological Research Council of Türkiye (TÜBİTAK).

**Data availability** The data presented in this study are available on request from the corresponding author.

## Declarations

**Conflict of interest** There are no conflicts to declare.

**Ethical approval** No ethical approval was required for this research as it did not involve human tissue or any other parts of living organisms.

**Open Access** This article is licensed under a Creative Commons Attribution 4.0 International License, which permits use, sharing, adaptation, distribution and reproduction in any medium or format, as long as you give appropriate credit to the original author(s) and the source, provide a link to the Creative Commons licence, and indicate if changes were made. The images or other third party material in this article are included in the article's Creative Commons licence, unless indicated otherwise in a credit line to the material. If material is not included in the article's Creative Commons licence and your intended use is not permitted by statutory regulation or exceeds the permitted use, you will need to obtain permission directly from the copyright holder. To view a copy of this licence, visit <http://creativecommons.org/licenses/by/4.0/>.

## References

1. A.K. Kapuscinska, M. Kwoka, M.A. Borysiewicz, T. Wojciechowski, N. Licciardello, M. Sgarzi, G. Cuniberti, Photocatalytic degradation of methylene blue at nanostructured ZnO thin films. *Nanotechnology* **34**, 155702 (2023)
2. K. Qi, B. Cheng, J. Yu, W. Ho, Review on the improvement of the photocatalytic and antibacterial activities of ZnO. *J. Alloy. Compd.* **727**, 792–820 (2017)
3. M. Sathya, G. Selvan, M. Karunakaran, K. Kasirajan, S. Usha, M. Logitha, S. Prabhakaran, P. Baskaran, Synthesis and characterization of cadmium doped on ZnO thin films prepared by SILAR method for photocatalytic degradation properties of MB under UV irradiation. *Eur. Phys. J. Plus* **138**, 67 (2023)
4. A. Mahroug, I. Mahroug, S. Berra, D. Allali, S. Hamrit, A. Guelil, A. Zoukel, S. Ullah, Optical, luminescence, photocurrent and structural properties of sol-gel ZnO fibrous structure thin films for optoelectronic applications: a combined experimental and DFT study. *Opt. Mater.* **142**, 114043 (2023)
5. A.C. Badgujar, B.S. Yadav, G.K. Jha, S.R. Dhage, Room temperature sputtered aluminum-doped ZnO thin film transparent electrode for application in solar cells and for low-band-gap optoelectronic device. *ACS Omega* **7**, 14203–14210 (2022)
6. K.K. Jasmi, T.A. Johnny, V.S. Siril, K.N. Madhusoodanan, Influence of defect density states on  $\text{NO}_2$  gas sensing performance of Na: ZnO thin films. *J. Sol-Gel Sci. Technol.* (2023). <https://doi.org/10.1007/s12034-022-02798-y>
7. K.M. Sandeep, S. Bhat, S.M. Dharmaprakash, Structural, optical, and LED characteristics of ZnO and Al doped ZnO thin films. *J. Phys. Chem. Solids* (2017). <https://doi.org/10.1016/j.jpcs.2017.01.003>
8. F. Güell, A. Galdámez-Martínez, P.R. Martínez-Alanis, A.C. Catto, F. da Luís, V.R. Silva, G.S. Mastelaro, A. Dutt, ZnO-based nanomaterials approach for photocatalytic and sensing applications: recent progress and trends. *Mater. Adv.* **4**, 3685–3707 (2023)
9. S. Karakaya, Mg Katkılı ZnO Filmlerinin Üretimi ve Karakterizasyonu. *J. Sci. Eng.* (2017). <https://doi.org/10.21205/deufmd.2017195648>
10. P. Khosravi, S.A. Seyyed Ebrahimi, Structural, electrical and optical characterization of ZnO: Li thin films prepared by sol-gel spin coating. *J. Ultrafine Grained Nanostruct. Mater.* **56**(1), 108–120 (2023)



11. M.H. Fernandes, B. Ramos, A. Luiz da Silva, D. Gouvea, Chloride-doped ZnO thin films prepared by spray pyrolysis: effects on microstructural, optical, and photocatalytic properties. *Micro Nanostruct.* **177**, 207550 (2023)
12. Y. Tsai, N. Wang, C.-L. Tsai, Fluorine-doped ZnO transparent conducting thin films prepared by radio frequency magnetron sputtering. *Thin Solid Films* **518**, 4955–4959 (2010)
13. S. Rafique, A.K. Kasi, J.K. Aminullah, M. Kasi, Z.S. Bokhari, Fabrication of Br doped ZnO nanosheets piezoelectric nanogenerator for pressure and position sensing applications. *Curr. Appl. Phys.* **21**, 72–79 (2021)
14. A.T.T. Pham, N.M. Ngo, O.K.T. Le, D.V. Hoang, T.H. Nguyen, T.B. Phan, V.C. Tran, High-mobility sputtered F-doped ZnO films as good-performance transparent-electrode layers. *J. Sci. Adv. Mater. Devices* **6**, 446–452 (2021)
15. M.N.H. Liton, A. Rani, M.K.R. Khan, M.S.I. Sarker, M.M. Rahman, M. Kamruzzman, Insight of the role of F-impurity on the structural, electro-optical properties of ZnO: DFT and experiment. *Mater. Sci. Semicond. Process.* **154**, 107223 (2023)
16. B. Paramanik, S. Samanta, D. Das, Near room-temperature synthesis of transparent conducting fluorine-doped ZnO thin films as window layer for solar cells. *Opt. Mater.* **133**, 112961 (2022)
17. T. Hurma, M. Caglar, Effect of anionic fluorine incorporation on structural, optical and electrical properties of ZnO nanocrystalline films. *Mater. Sci. Semicond. Process.* **110**, 104949 (2020)
18. K. Bahedi, M. Addou, A. Mrigal, H. Cherrad, Z. Soufiani, S. Bayoud, H. Fatouhi, Z. El Jouad, A. Ihlal, H. Kirou, Nonlinear optical characteristics and photoluminescence of sprayed deposited ZnO: F thin films. *Mater. Today Proc.* **24**, 91–94 (2020)
19. C.-C. Chen, F.-H. Wang, S.-C. Chang, C.-F. Yang, Using oxygen plasma pretreatment to enhance the properties of F-doped ZnO films prepared on polyimide substrates. *Materials* **11**, 1501 (2018)
20. A.A. Galil, M.S.A. Hussien, I.S. Yahia, Synthesis and optical analysis of nanostructured F-doped ZnO thin films by spray pyrolysis: transparent electrode for photocatalytic applications. *Opt. Mater.* **114**, 110894 (2021)
21. G. Vitiello, G. Iervolino, C. Imparato, I. Rea, F. Borbone, L. De Stefano, A. Aronne, V. Vaiano, F-doped ZnO nano- and mesocrystals with enhanced photocatalytic activity in diclofenac degradation. *Sci. Total. Environ.* **762**, 143066 (2021)
22. N.P. Subiramaniam, S. Vadivel, S. Kumaresan, K. Vallalperuman, Fluorine-doped nanocrystalline ZnO powders prepared via microwave irradiation route as effective materials for photocatalyst. *J. Mater. Sci. Mater. Electron.* **28**, 16173–16180 (2017)
23. M.W. Kadi, D. McKinney, R.M. Mohamed, I.A. Mkhallid, W. Sigmund, Fluorine doped zinc oxide nanowires: enhanced photocatalysts degrade malachite green dye under visible light conditions. *Ceram. Int.* **42**, 4672–4678 (2016)
24. L.R. Salaya, A.H. Ramírez, L.H. Reyes, J.L.G. Mar, M.V. Rodríguez, E.S. Cervantes, Solar photocatalytic degradation of diclofenac aqueous solution using fluorine doped zinc oxide as catalyst. *J. Photochem. Photobiol. A Chem.* **391**, 112364 (2020)
25. S. Karakaya, *An evaluation of the relationship between physical properties and photocatalytic performance of ZnO coatings* (Gece Publishing, 2022)
26. S. Karakaya, L. Kaba, Enhancing the photocatalytic performance of ZnO: Gd films produced by spray pyrolysis using methylene blue pollutant. *J. Mater. Sci. Mater. Electron.* **34**, 1295 (2023)
27. G. Kaur, A. Mitra, K.L. Yadav, Pulsed laser deposited Al-doped ZnO thin films for optical applications. *Progress Nat. Sci. Mater. Int.* **25**, 12–21 (2015)
28. A. Kompa, B.L. Devi, U. Chaitra, Determination of optical constants of vacuum annealed ZnO thin films using Wemple Di DOMENICO model, Sellmeyer's model and Miller's generalized rules. *Mater. Chem. Phys.* **299**, 127507 (2023)
29. V. Şenay, Some physical properties of nanostructured Al doped ZnO thin films synthesized by RF magnetron sputtering at room temperature. *J. Mater. Sci. Mater. Electron.* **30**, 9910–9915 (2019)
30. A. Diha, S. Benramache, L. Fellah, The Crystalline structure, optical and conductivity properties of fluorine doped ZnO nanoparticles. *J. Nano- Electron. Phys.* **11**(3), 03002 (2019)
31. N.E. Sung, S.W. Kang, H.J. Shin, H.K. Lee, I.J. Lee, *Thin Solid Films* **547**, 285 (2013)
32. K. Natu, V.K. Kaushik, M. Laad, Optical and structural characterization of aerosol-assisted CVD-grown Ni:ZnO thin films. *J. Korean Phys. Soc.* (2023). <https://doi.org/10.1007/s40042-023-00809-7>
33. O. Karzazi, L. Soussi, A. Louardi, A. El Bachiri, M. Khaidar, M. Monkade, H. Erguig, M. Taleb, Transparent conducting properties of Mg and Al co-doped ZnO thin films deposited by spray pyrolysis technique. *Superlattices Microstruct.* **127**, 61–65 (2019)
34. A.T. Nomaan, A.A. Ahmed, N.M. Ahmed, M.I. Idris, M.R. Hashim, M. Rashid, ZnO quantum dot based thin films as promising electron transport layer: influence of surface-to-volume ratio on the photoelectric properties. *Ceram. Int.* **47**, 12397–12409 (2021)
35. M.M.H. Farooqi, R.K. Srivastava, Effect of annealing temperature on structural, photoluminescence and photoconductivity properties of ZnO thin film deposited on glass substrate by Sol–Gel spin coating method. *Proc. Natl. Acad. Sci. India Sect. A Phys. Sci.* **90**(5), 845–859 (2020)
36. S. Karakaya, S. Kurtaran, Physical properties of ZnO:B: Ce nanofiber like thin films prepared by ultrasonic spray pyrolysis technique. *Inorg. Chem. Commun.* **153**, 110747 (2023)
37. S. Rajeh, A. Mhamdi, S. Ben Ameer, A. Arfaoui, G. Leroy, B. Duponchel, S. Guermazi, Enhancement of visible light emission of ni-doped ZnO sprayed thin films by copper co-doping, ISSN 2070–2051. *Prot. Met. Phys. Chem. Surf.* (2023). <https://doi.org/10.1134/S2070205123700533>
38. K. Ravichandran, N. Dineshbabu, T. Arun, C. Ravidhas, S. Valanarasu, Effect of fluorine (an anionic dopant) on transparent conducting properties of Sb (a cationic) doped ZnO thin films deposited using a simplified spray technique. *Mater. Res. Bull.* **83**, 442–452 (2016)
39. K. Ravichandran, N.S. Jyothi, K. Thirumurugan, S. Suvathi, N. Chidhambaram, R. Uma, B. Sundaresan, Influence of Mo + F incorporation and point of zero charge on the dye degradation efficiency of ZnO thin films. *Chem. Phys.* **564**, 111714 (2023)
40. S.S. Shinde, P.S. Shinde, S.M. Pawar, A.V. Moholkar, C.H. Bhosale, K.Y. Rajpure, Physical properties of transparent and conducting sprayed fluorine doped zinc oxide thin films. *Solid State Sci.* **10**, 1209–1214 (2008)
41. H. Shen, X. Shi, Z. Wang, Z. Hou, C. Xu, L. Duan, X. Zhao, H. Wu, Defects control and origins of blue and green emissions in sol-gel ZnO thin films. *Vacuum* **202**, 111201 (2022)
42. S. Berra, A. Mahroug, S. Hamrit, M.A. Azmin, A. Zoukel, S. Berri, N. Selmi, Experimental and DFT study of structural and optical properties of Ni-doped ZnO nanofiber thin films for optoelectronic applications. *Opt. Mater.* **134**, 113188 (2022)
43. H. Qian, L. Xu, F. Xian, J. Su, X. Luo, Accelerating the formation of high-quality optical surface layer in ZnO thin films by the increase of heat-treatment temperature. *Optik* **232**, 166527 (2021)
44. P. Manzhi, R. Kumari, Md.B. Alam, G.R. Umapathy, R. Krishna, S. Ojha, R. Srivastava, O.P. Sinha, Mg-doped ZnO nanostructures for efficient organic light emitting diode. *Vacuum* **166**, 370–376 (2019)
45. C.-Y. Chang, J. Shieh, Y.-L. Kuo, J.-Y. Guo, S.-Y. Chen, C.-L. Kuo, Tuning lattice defects and photocurrent response of ZnO thin films by Mg doping and Ar-H<sub>2</sub> atmospheric plasma treatment. *Appl. Surf. Sci.* **638**, 158018 (2023)

46. R. Peña-García, Y. Guerra, R. Milani, D.M. Oliveira, A.R. Rodrigues, E. Padrón-Hernández, The role of Y on the structural, magnetic and optical properties of Fe-doped ZnO nanoparticles synthesized by sol gel method. *J. Magn. Magn. Mater.* **498**, 166085 (2020)
47. F. Ghahramanifard, A. Rouhollahi, O. Fazlolahzadeh, Electrodeposition of Cu-doped p-type ZnO nanorods; effect of Cu doping on structural, optical and photoelectrocatalytic property of ZnO nanostructure. *Superlattices Microstruct.* **114**, 1–14 (2018)
48. Z.R. Khan, M.S. Khan, M. Zulfequar, M.S. Khan, Optical and structural properties of ZnO thin films fabricated by sol-gel method. *Mater. Sci. Appl.* **2**, 340–345 (2011)
49. M. Ashokkumar, M. Rajkumar, K.S. Pugazhivadivu, Assessment of properties, photocatalytic activity, cytotoxicity, and antibacterial activity of (Cu, Cr) dual-doped ZnO nanoparticles. *J. Inorg. Organomet. Polym. Mater.* (2023). <https://doi.org/10.1007/s10904-023-02730-9>
50. A.A. Aboud, A. Mukherjee, M. AlDossari, N.S.A.E. Gawaad, A.M. Saad, Pure and co-doped ZnO nano-sheets thin films as UV detectors. *J. Mater. Sci. Mater. Electron.* **34**, 1344 (2023)
51. A. Omerzu, R. Peter, D. Jardas, I. Turel, K. Salamon, M. Podlogar, D. Vengust, I.J. Badovinac, I.K. Piltaver, M. Petravic, Large enhancement of photocatalytic activity in ZnO thin films grown by plasma-enhanced atomic layer deposition. *Surfaces Interfaces* **23**, 100984 (2021)
52. A. Kamal, M.H. Saleem, H. Alshaya, M.K. Okla, H.J. Chaudhary, M.F.H. Munis, Ball-milled synthesis of maize biochar-ZnO nanocomposite (MB-ZnO) and estimation of its photocatalytic ability against different organic and inorganic pollutants. *J. Saudi Chem. Soc.* **26**, 101445 (2022)
53. G.M. Nam, M.S. Kwon, F-doped ZnO by sol-gel spin-coating as a transparent conducting thin film. *Electron. Mater. Lett.* **7**(2), 127–131 (2011)

**Publisher's Note** Springer Nature remains neutral with regard to jurisdictional claims in published maps and institutional affiliations.